Theory and Practical Procedure for Predicting S-N Curves at Various Stress Ratios#

Ho Sung Kim*

Mechanical Engineering, School of Engineering, Faculty of Engineering and Built Environment, The University of Newcastle, Callaghan, NSW 2308, Australia

Abstract: Predictive models in the past for stress ratio effect on S-N fatigue life have been subject to modifications since the 19th century. Many of them have been developed with limited experimental verifications or beyond the theoretical limit. Also, they have employed weak S-N curve models for the development, resulting in inefficiency in applications. There has been, also, a missing link in the development of predictive models between S-N curve behaviour and stress ratio effect. In this paper, theoretical analysis is presented and subsequently a practical procedure for predicting S-N curves at various stress ratio is proposed. The theoretical and experimental characteristics of the constant fatigue life (CFL) diagram were clarified for capability and limitations, and dependence of experimental fatigue behaviour. Mathematical relationships between linear CFL lines and fatigue damage parameters were successfully derived. As a result, the Kim and Zhang S-N curve model was successfully dovetailed with the linear CFL lines to predict S-N curves for the whole range of stress ratios. Theoretical predictions of fatigue life based on the mathematical relationships were verified with experimental data.

Keywords: S-N fatigue, Constant fatigue life, Stress ratio, Fatigue damage.

1. INTRODUCTION

Fatigue is a damage process leading to structural failures. There have been two different approaches for the fatigue failures for structural materials. One of the approaches is based on the analysis of individual cracks using fracture mechanics parameters such as the stress intensity factor [1]. The other approach is based on the collective analysis of "small" multiple cracks [2, 3] using the S-N curve characteristics, including crack initiation at an un-notched geometry. (S and N in the acronym stand for stress and number of fatigue loading cycles at failure respectively.)

The S-N fatigue studies in history have been somewhat disorderly in sequence as already pointed out by Burhan and Kim [4]. For example, the research of stress ratio effect on fatigue life [5-8] mostly appears earlier than that of S-N curve modelling [9-11] although S-N curve modelling should be a prior task to the stress ratio effect for fatigue life prediction. One would be surprised to find the fact that the stress ratio effect modelling for fatigue life prediction has still been a contemporary research topic since the 19th century. It would not be surprising, however, to find the fact that the knowledge advancement in the area has been slow. The earlier disorderly sequence of events has still been continued. For example, some researchers [12, 13] have already progressed on to the research on S-N fatigue life prediction for the variable amplitude loading while some other researchers [14, 15] have still been grappling with developing constant fatigue life (CFL) models for the stress ratio effect under the constant amplitude loading. Furthermore, the original contributions have often been improperly interpreted and used by many researchers as already pointed out by Sendeckyj [16]. For example, the constant fatigue life (CFL) diagrams have been called Goodman diagrams [17]. In fact, Gerber [5] published in 1874 the CFL diagram consisting of σ_{max}/σ_u versus σ_{min}/σ_u (σ_{max}, σ_{min}, and σ_u: applied peak stress, valley stress, and ultimate strength respectively) followed by Goodman in 1899 [7] for a similar graphical representation of experimental data. Haigh in 1917 [18] may be the first to present the linear expression between stress amplitude (σ_a) and mean stress (σ_{mean}) for a particular material *i.e.* $\sigma_{-1}\left(1-\sigma_{mean}/\sigma_u\right)$ where σ_{-1} is the fatigue limit at stress ratio (R)=-1, but has erroneously been called the Goodman relation. Further, it has been found that some formulations had been developed erroneously and used. For example, some researchers [19] proposed an S-N curve expression as a function of *R* but by replacing the stress range ($\Delta\sigma$) with σ_{max} (1-R), which does not affect the nature of the original expression, given that $\Delta\sigma = \sigma_{max}$ (1-R) is no more than a definition of R. Some researchers presented something beyond understanding for CFL model verification such that they plotted some fatigue experimental values of

*Address correspondence to this author at the Mechanical Engineering, School of Engineering, Faculty of Engineering and Built Environment, The University of Newcastle, Callaghan, NSW 2308, Australia: Tel: +61 2 4921 6211;
E-mail: ho-sung.kim@newcastle.edu.au

Part of this paper was submitted to the Fatigue Design 2019, 8th edition of the International conference on fatigue design, 20&21 November 2019, Senlis, France; and published in Procedia Structural Integrity 19(2019), pp.472-81.

E-ISSN: 2312-5470/19 © 2019 Savvy Science Publisher

σ_a at failure, whose values of $|\sigma_{min}|$ as ones that are larger than the compressive strength on a CFL diagram [20].

It may be obvious that, to predict the fatigue life at different stress ratios, two sets of characteristics may need to be understood *i.e*. one for S-N curve behaviour and the other for CFL at various stress ratios. In other words, the fatigue life (N_f) is a function of two independent variables *i.e*. applied stress and *R*. The applied peak stress (σ_{max}) may be taken as the first variable at a given *R*, which may be accommodated in an S-N curve model. The other variable *R* may be accommodated in a CFL model at a CFL. The individual models for respective S-N curve behaviour and stress ratio effect on fatigue life are once validly established, a relationship between the two independent variables should be found. A different approach, of course, may be possible as have been attempted with a single equation for accommodating the two independent variables (R and σ_{max}) on a trial and error basis [19, 21, 22]. The S-N curve models at a constant *R* in such an approach, however, were found to be inferior in the first place to those developed as a function of single variable (σ_{max}) [4]. Burhan and Kim [4] evaluated most of the S-N curve models available since 1910. They found that three S-N curve models separately proposed by Weibull [23], Sendeckyj [11], and Kim and Zhang [24] are the most adequately represent the materials characteristics for the whole range of stress ratios. Ironically, however, none of the three models have been much used for developing a predictive model for fatigue life at different stress ratios. They also found that the Kim and Zhang model among the three models has an advantage of having an analytical relationship with the fatigue damage rate [3].

CFL models unlike S-N curve models have been evolved with a limited applicability following the numerous early models developed for fatigue limit design as reviewed by Sendeckyj [16]. Simultaneously, they have continually been subject to modifications for generality as the CFL models encounter the difficulty of application. Main reasons for this may include limited theoretical understanding of CFL diagram on σ_{mean} versus σ_a plane, and discrepancy between assumption and real experimental fatigue behaviour. For example: (a) fatigue characteristics caused by discrepancy between compressive and tensile loadings were not reflected, producing symmetrical CFL lines [14, 25]; (b) materials were assumed to fail always at a constant mean stress at *R*=1 independent of any other applied stress levels lower than σ_{uT} [15, 26]; and (c) boundary conditions (or applicable R range – *e.g*. R=−1 as a boundary) were arbitrarily defined irrespective of fatigue characteristics formed due to discrepancy between compressive and tensile strengths [20].

The ultimate purpose of this paper was to propose a practical procedure for predicting S-N curves at any stress ratio for materials subjected to uniaxial fatigue loading. To this end, and in the light of the deficiencies in the previous studies, the CFL diagram characteristics were clarified for both theoretical and experimental aspects. Subsequently, explicit analytical expressions for damage parameters as functions of two independent variables (*i.e*. applied peak stress and stress ratio) were derived, allowing us to predict S-N curves.

2. A NEW PROPOSED THEORY AND PROCEDURE FOR FATIGUE LIFE PREDICTION

The following proposed theory is for determining the damage parameters as functions of stress ratios, leading to a practical procedure for predicting S-N curves at various stress ratios.

2.1. An S-N Curve Model to be Employed

A valid S-N curve model is a prerequisite for predicting fatigue lives at various stress ratios. An S-N curve model developed by Kim and Zhang [24, 27] may be advantageous compared to other models [4] because of an analytical relationship with fatigue damage rate.

The Kim and Zhang S-N curve model was developed by quantifying the fatigue damage at tensile fatigue failure (D_{fT}),

$$D_{fT} = 1 - \frac{\sigma_{max}}{\sigma_{uT}} \tag{1a}$$

or the fatigue damage at compressive fatigue failure (D_{fC}),

$$D_{fC} = 1 - \frac{|\sigma_{min}|}{|\sigma_{uC}|} \tag{1b}$$

where σ_{max} = applied peak stress, σ_{min} = applied valley stress, σ_{uT} = ultimate tensile strength, σ_{uC} = ultimate compressive strength. Note these equations satisfy the requirement for D_f quantification [3, 28]. It has been found that experimental fatigue damage rates follow

$$\frac{\partial D_{fT}}{\partial N_f} = \alpha(\sigma_{max})^{\beta} \tag{2a}$$

or

$$\frac{\partial D_{fC}}{\partial N_f} = \alpha|\sigma_{min}|^{\beta} \quad (2b)$$

where α, β = damage rate fitting parameters, and N_f = number of cycle at failure. The number of cycles at failure (N_f) in this equation can be obtained by integration, yielding an S-N curve as a function of applied peak stress (σ_{max}) in the case of tension dominant failure:

$$N_f = \frac{(\sigma_{uT})^{-\beta}}{\alpha(\beta-1)}\left[\left(\frac{\sigma_{max}}{\sigma_{uT}}\right)^{1-\beta} - 1\right] + N_0; \quad (3a)$$

or as a function of valley stress (σ_{min}) in the case of compression dominant failure,

$$N_f = \frac{|\sigma_{uC}|^{-\beta}}{\alpha(\beta-1)}\left(\left|\frac{\sigma_{min}}{\sigma_{uC}}\right|^{1-\beta} - 1\right) + N_0. \quad (3b)$$

These equations are invertible such that:

$$\sigma_{max} = \sigma_{uT}\left(\frac{\alpha(\beta-1)(N_f-N_0)}{(\sigma_{uT})^{-\beta}} + 1\right)^{\frac{1}{1-\beta}} \quad (4a)$$

or

$$|\sigma_{min}| = |\sigma_{uC}|\left(\frac{\alpha(\beta-1)(N_f-N_0)}{|\sigma_{uC}|^{-\beta}} + 1\right)^{\frac{1}{1-\beta}}. \quad (4b)$$

The term N_0 in each equation is to adjust the initial number of cycles for the first cycle failure point [3]. For example, N_0=0.5 cycle at $\sigma_{max} = \sigma_{uT}$ with R=0. The fitting parameters (α and β) for S-N curve in Equation (3) are identical to those for damage rate at failure with respect to N_f [Equation (2)]. The two parameters (α and β) can be numerically determined for a set of fatigue data at a given stress ratio using

$$\frac{\Delta D_{fT(i)}}{\Delta N_{f(i)}} \approx \alpha\left(\sigma_{\max(i)}\right)^{\beta} \quad (5a)$$

or

$$\frac{\Delta D_{fC(i)}}{\Delta N_{f(i)}} \approx \alpha\left|\sigma_{\min(i)}\right|^{\beta}. \quad (5b)$$

For tensile failure mode, subscript i = 1,2,3,… for different stress levels ($\sigma_{max(i)}$) may be used for numerical calculation *i.e.* $\Delta D_{fT(i)} = D_{fT(i-1)} - D_{fT(i)}$ for $D_{fT(i-1)} > D_{fT(i)}$ or $|1 - \sigma_{max(i-1)}/\sigma_{uT}| > |1 - \sigma_{max(i)}/\sigma_{uT}|$, $\Delta N_{f(i)} = N_{f(i-1)} - N_{f(i)}$ for $N_{f(i-1)} > N_{f(i)}$, and $\sigma_{max(i)} = (\sigma_{max(i)} - \sigma_{max(i-1)})/2$. A collected data set for $\log(\Delta D_{fT(i)}/\Delta N_{fT(i)})$ may be plotted as a function of $\log \sigma_{max(i)}$ such that β is the slope and 10^{α} is an intercept. A best fit polynomial equation for experimental S-N data may be used for converting into the numerical values, and then for finding α and β with $\Delta D_{fT(i)}/\Delta N_{fT(i)}$ and $\sigma_{max(i)}$. For compressive failure mode, a similar process can be adopted after replacing $\sigma_{max(i)}$ with $|\sigma_{min(i)}|$, $\Delta D_{fT(i)}$ with $\Delta D_{fC(i)}$, etc.

2.2. Characteristics of Constant Fatigue Life (CFL) Diagram

The constant fatigue life (CFL) diagram on the plane of mean stress (σ_{mean}) versus alternating stress (σ_a) (Figure **1**) is useful not only for providing information of fatigue lives in relation with stress ratios but also for predicting S-N curves at various stress ratios. It consists of ordinate for σ_a, abscissa for σ_{mean}, radial lines emanating from the origin for constant stress ratios, and CFL lines. The CFL lines may be decomposed into two sets. One of the sets which hereafter will be referred to as the *first cycle CFL* lines can be theoretically identified using the quasi-static ultimate compressive (σ_{uC}) and tensile (σ_{uT}) strengths. The other set of CFL lines (which hereafter will be referred to as *fatigue CFL* lines) depends on the experimental fatigue behaviour (Figure **2**). In the case of fibre reinforced composites, yield strength (σ_y) and ultimate strength (σ_u) are approximately equal unlike the monolithic ductile materials. However, σ_y may be preferably used for monolithic ductile materials as suggested by Soderberg [8] depending on the definition of failure.

2.2.1. The First Cycle CFL Lines

The first cycle CFL lines are a locus of failure points within the first load cycle (about 0.5 cycle between 0.25 to 0.75 cycles). It can be intuitively found from the schematic load cycling at different stress ratios as shown in Figure **1**. The dot in each load cycle in Figure **1** represents a failure point corresponding to either σ_{uC} *or* σ_{uT}. For example, the failure point at R=0 is found to be $\sigma_{\max} = \sigma_{uT}$ and N_f=0.5 cycle. Thus, the first cycle CFL lines consists of two straight lines forming an isosceles right triangle for approximately linear relationships between σ_a and σ_{mean} for each half of the triangle for the whole range of stress ratios. The location of the isosceles triangle apex is found to be

$$\sigma_a = \frac{\sigma_{uT} + |\sigma_{uC}|}{2} \quad (6)$$

and

$$\sigma_{mean} = \frac{\sigma_{uT} - |\sigma_{uC}|}{2}. \quad (7)$$

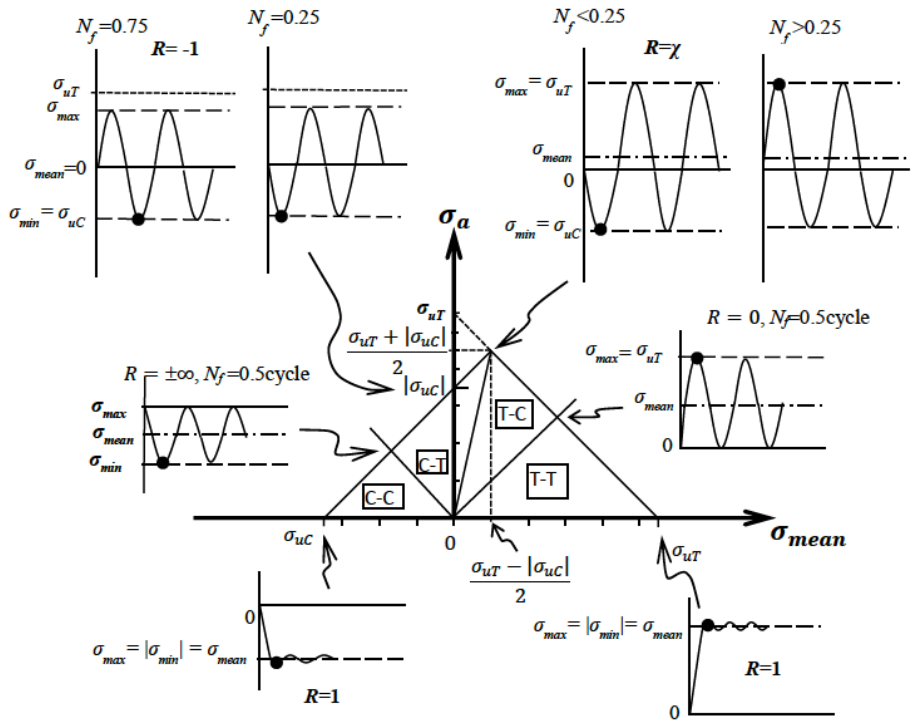

(a)

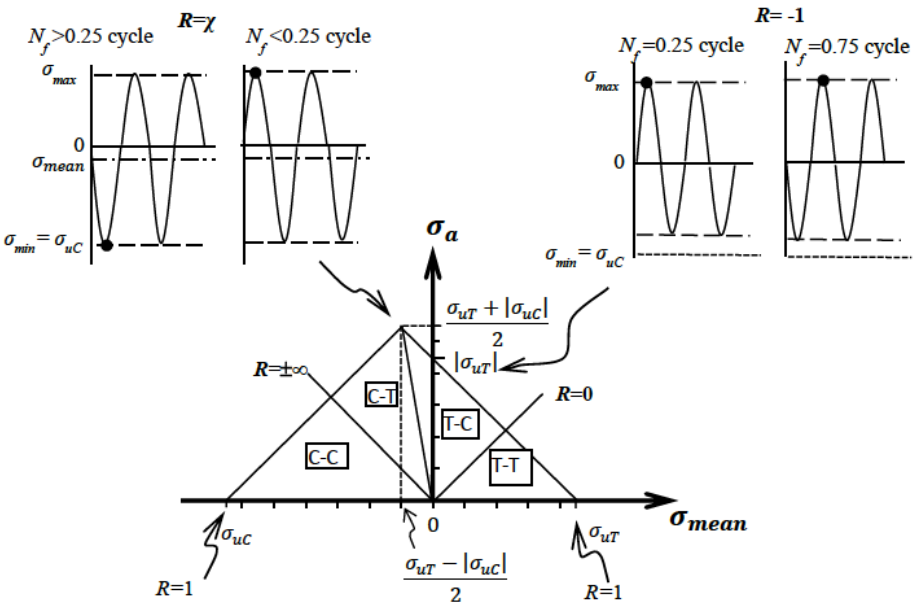

(b)

Figure 1: CFL diagrams for the first cycle CFL lines with corresponding loading points: (**a**) for $\sigma_{uT} > |\sigma_{uC}|$; and (**b**) for $\sigma_{uT} < |\sigma_{uC}|$.

Accordingly, the location of σ_{mean} for the triangle apex depends on the static strengths. If $\sigma_{uT} > |\sigma_{uC}|$, then $\sigma_{\max} = (\sigma_{uT} - |\sigma_{uC}|)/2 > 0$ as shown Figure **1a**; and if $\sigma_{uT} < |\sigma_{uC}|$, then $\sigma_{mean} = (\sigma_{uT} - |\sigma_{uC}|)/2 < 0$ as shown Figure **1b**. Thus, the stress ratio of the radial line passing through the apex (R_χ or χ) is found to be

$$R_\chi = \chi = \frac{\sigma_{mean} - \sigma_a}{\sigma_{mean} + \sigma_a} = \frac{-|\sigma_{uC}|}{\sigma_{uT}} \tag{8}$$

and its slope (S_χ) is also found to be

$$S_\chi = \frac{\sigma_{uT} + |\sigma_{uC}|}{\sigma_{uT} - |\sigma_{uC}|}. \tag{9}$$

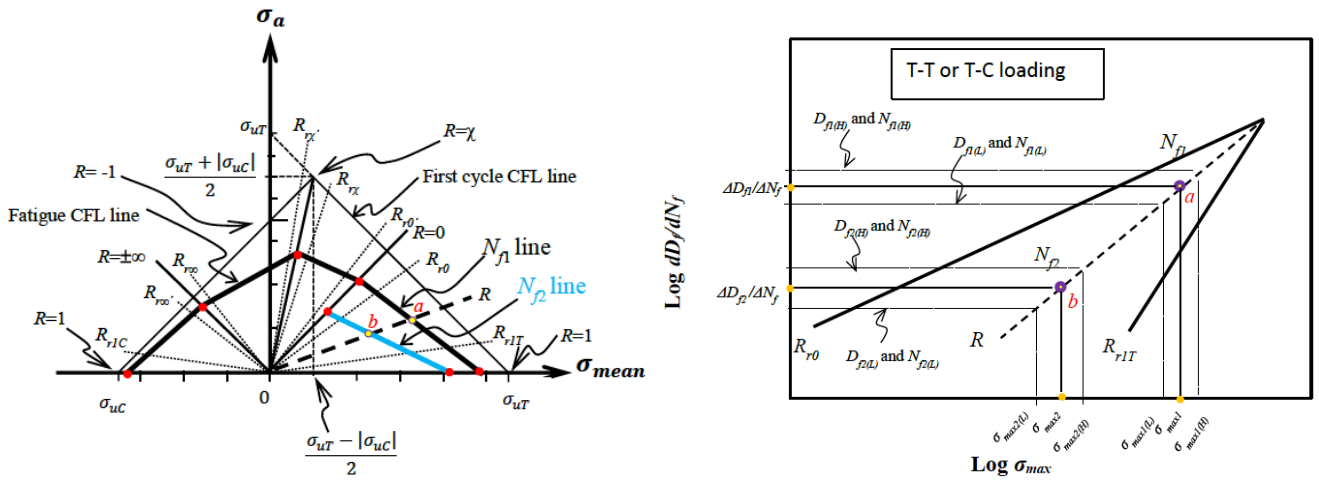

(**a**) (**b**)

Figure 2: Diagrams for notation: (**a**) fatigue CFL lines for $\sigma_{uT} > |\sigma_{uC}|$; and (**b**) log ($dD_f/dN_f$) versus log$\sigma_{max}$ at a given R with points a and b, corresponding to those points in fatigue CFL diagram in '(a)'.

The critical stress ratio (χ) as seen indicates a location for the transition of the first cycle CFL line slope dictated by the static strengths. The first cycle CFL line on the right side of $R=\chi$ is due to the mean loading $\sigma_{mean} > \left(\sigma_{uT} - |\sigma_{uC}|\right)/2$ generating the failure in tension mode, while that of left side of the radial line at $R=\chi$ is due to the mean loading $\sigma_{mean} < \left(\sigma_{uT} - |\sigma_{uC}|\right)/2$, generating the failure in compression mode.

The intercept value on σ_a-axis of the first cycle CFL line is found to be $|\sigma_{uC}|$ if $\sigma_{uT} > |\sigma_{uC}|$ (Figure **1a**) or $|\sigma_{uT}|$ if $\sigma_{uT} < |\sigma_{uC}|$ (Figure **1b**).

Thus, the first cycle CFL lines is theoretically determined once the static strengths are given. If a set of experimental results would not conform to the theoretical description here, the experiment may be judged to be erroneously conducted [29].

2.2.2. Fatigue CFL Lines

Unlike the first cycle CFL lines, we do not know how CFL lines look like until the experimental fatigue data sets at different stress ratios are available. We do know, however, that the two distinctive types of static loading for the first cycle are subdivided into further four distinctive types of loading for the fatigue CFL lines dependent of mean stress. They may be represented by the four stress ratio ranges according to the diagrams in Figure **1**, *i.e.* $0 \le R \le 1$ and $\chi \le R \le 0$ when subjected to the mean loading, $\sigma_{mean} \le \left(\sigma_{uT} - |\sigma_{uC}|\right)/2$; and $\pm\infty \le R \le \chi$ and $\pm\infty \le R \le 1$ when subjected to the mean loading, $\sigma_{mean} \le \left(\sigma_{uT} - |\sigma_{uC}|\right)/2$. The fatigue damage at a stress range $0 \le R < 1$ is due to tension-tension (T-T) loading; $\chi \le R \le 0$ is due to tension-compression (T-C) loading; $\pm\infty \le R \le \chi$ is due to compression-tension (C-T) loading; and $\pm\infty \le R \le 1$ is due to compression-compression (C-C) loading. The experimental observation suggests a damage mechanism transition occurs when the loading condition changes [30] although the failure modes (*e.g.* tensile and compressive failures) at four different stress ratio ranges coincide with those of the first cycle loading according to the experimental findings [26]. Accordingly, the fatigue CFL lines are expected to be affected by the loading type. Nonetheless, the approximate linearity in the first cycle CFL lines occurred in either side of χ may continue until the substantial fatigue damage occurs. It may, then, start to be affected by the loading type and a majority of experimental data sets indicate that the fatigue CFL lines within each range of stress ratios under one of four loading types are approximately linear. Accordingly, if the fatigue CFL lines are assumed to be linear in each stress ratio range as shown in Figure **2**, they can be theoretically calculated using an appropriate number of sets of experimental fatigue data at different reference stress ratios to find the damage parameters (α and β) in Equations (2-5) for predicting S-N curves. The fatigue CFL line at R=1 for either T-T loading or C-C loading is in general not equal to each static strength point (σ_{uT} or σ_{uC}) [31, 32] despite the fact that most existing predictive models assume that it is equal to the static strength point (Figure **2**). This can easily be realised by converting the number of loading cycles (N_f) into time. Also, some difference in fatigue damage between C-C and T-T loadings is envisaged R=1 because the compressive loading tends to close

the cracks whereas the tensile loading tends to open the cracks producing more fatigue damage. Accordingly, distances between fatigue CFL lines and σ_{uC} at, or near, R=1 under C-C loading are closer than those between fatigue CFL lines and σ_{uT} under T-T loading.

The fatigue CFL lines may be formulated for the four different loading types. The four area segments indicated by the corresponding four loading types in CFL diagram (Figure **1**) are four domains from the multi-variable mathematics point of view, each of which is with boundary conditions produced by two sets of reference experimental data (TRED) and the first cycle CFL line.

For a stress ratio range, $0 \le R < 1$ (T-T loading), stress ratios for TRED (*i.e.* R_{r0} and R_{r1T}) should be $0 \le R < R_{r0} < R \le R_{r1T} < 1$ as schematically shown in Figure **2**, where R is any chosen stress ratio at which an S-N curve is to be theoretically calculated for prediction. It is noted that the reference stress ratio, R_{r0} is close to R=0, and R_{r1T} is close to R=1. The slopes (S_{r0} and S_{r1T}) of the radial lines for respective R_{r0} and R_{r1T} are found to be

$$S_{r0} = \frac{1-R_{r0}}{1+R_{r0}} \tag{10}$$

and

$$S_{r1T} = \frac{1-R_{r1T}}{1+R_{r1T}} . \tag{11}$$

The slope of fatigue CFL line (S_R) or $S_{R(TT)}$ for T-T loading, intersecting the two radial lines at R_{r1T} and R_{r0} is found to be

$$S_{R(TT)} = \frac{S_{r0}\sigma_{mean,r0} - S_{r1T}\sigma_{mean,r1T}}{\sigma_{mean,r0} - \sigma_{mean,r1T}} , \tag{12}$$

such that the intercept at the ordinate (I) or $I_{(TT)}$ for T-T loading is found to be

$$I_{(TT)} = S_{r1T}\sigma_{mean,r1T} - S_R\sigma_{mean,r1T} . \tag{13}$$

Therefore,

$$\sigma_a = I_{(TT)} + S_{R(TT)}\sigma_{mean} . \tag{14}$$

For a stress ratio range, $\chi < R < 0$ (T-C loading), the same equations above for T-T loading can be used by replacing subscripts *i.e.* R_{r1T} with $R_{r0'}$, R_{r0} with $R_{r\chi}$, $\sigma_{mean,r0}$ with $\sigma_{mean,rx}$ and so on. Likewise, TRED obtained at two stress ratios (R_{rx} and $R_{r0'}$) as schematically shown in Figure **2** may be required for $\chi \le R \le R_{rx} < R < R_{r0'} \le R \le 0$. The reference stress ratio, R_{rx} is close to χ, and $R_{r0'}$ is close to R=0. The slopes (S_{rx} and $S_{r0'}$) of the radial lines for respective stress ratios $R_{r\chi}$ and $R_{r0'}$ are found to be

$$S_{r\chi} = \frac{1-R_{r\chi}}{1+R_{r\chi}} \tag{15}$$

and

$$S_{r0'} = \frac{1-R_{r_0'}}{1+R_{r_0'}} . \tag{16}$$

The slope of fatigue CFL line (S_R) or $S_{R(TC)}$ for T-C loading, intersecting the two radial lines at $R_{r0'}$ and $R_{r\chi}$ for both $|\chi|<1$ and $|\chi|>1$ is found to be

$$S_{R(TC)} = \frac{S_{r\chi}\sigma_{mean,r\chi} - S_{r0'}\sigma_{mean,r0'}}{\sigma_{mean,r\chi} - \sigma_{mean,r0'}} , \tag{17}$$

such that the intercept at the ordinate (I) or I_{TC} for T-C loading is also found to be

$$I_{(TC)} = S_{r0'}\sigma_{mean,r0'} - S_R\sigma_{mean,r0'} \tag{18}$$

Therefore,

$$\sigma_a = I_{(TC)} + S_R\sigma_{mean} . \tag{19}$$

For a stress ratio range, $-\infty < R < \chi$ (C-T loading), TRED obtained at two stress ratios ($R_{rx'}$ and $R_{r\infty}$) may be required for $-\infty \le R \le R_{r\infty} < R < R_{rx'} \le R \le \chi$. The slopes of the radial lines at $R = R_{rx'}$ and $R = R_{r\infty}$ are found to be

$$S_{r\chi'} = \frac{1-R_{r\chi'}}{1+R_{r\chi'}} \tag{20}$$

and

$$S_{r\infty} = \frac{1-R_{r\infty}}{1+R_{r\infty}} \tag{21}$$

respectively. The slope of fatigue CFL line (S_R) or $S_{R(CT)}$ for C-T loading, intersecting the two radial lines at $R_{r\chi'}$ and $R_{r\infty}$ for both $|\chi|<1$ and $|\chi|>1$ is found to be

$$S_{R(CT)} = \frac{S_{r\chi'}\sigma_{mean,r\chi'} - S_{r\infty}\sigma_{mean,r\infty}}{\sigma_{mean,r\chi'} - \sigma_{mean,r\infty}} , \tag{22}$$

so that the intercept of the fatigue CFL line at the ordinate (I) or $I_{(CT)}$ for C-T loading is found to be

$$I_{(CT)} = S_{r\infty}\sigma_{mean,r\infty} - S_{R(CT)}\sigma_{mean,r\infty} . \tag{23}$$

Therefore,

$$\sigma_a = I_{(CT)} + S_{R(CT)}\sigma_{mean} \cdot \quad (24)$$

For a stress ratio range, $+\infty \geq R > 1$ or $-\infty < R < 1$ (C-C loading), the same equations developed for C-T loading above can be used by replacing subscripts *e.g.* $R_{r\chi'}$ replaced by $R_{r\infty'}$, $R_{r\infty}$, replaced by R_{r1C}, and so on. Thus, TRED for $R_{r\infty'}$ and R_{r1C} may be required (Figure **2**) such that $+\infty \geq R \geq R_{r\infty'} > R > R_{r1C} \geq R > 1$, where R is any chosen stress ratio at which an S-N curve is theoretically calculated for prediction. The slope of fatigue CFL line (S_R) intersecting the radial line for $R_{r\infty'}$ for both $|\chi|<1$ and $|\chi|>1$ is found to be

$$S_{r\infty\prime} = \frac{1-R_{r\infty\prime}}{1+R_{r\infty\prime}} \quad (25)$$

and

$$S_{r1C} = \frac{1-R_{r1C}}{1+R_{r1C}} \quad (26)$$

respectively. The slope of fatigue CFL line (S_R) or $S_{R(CC)}$ for C-C loading, intersecting the two radial lines at $R_{r\infty'}$ and R_{r1C} for both $|\chi|<1$ and $|\chi|>1$ is found to be

$$S_{R(CC)} = \frac{S_{r\infty\prime}\sigma_{mean,r\infty\prime} - S_{r1C}\sigma_{mean,r1C}}{\sigma_{mean,r\infty\prime} - \sigma_{mean,r1C}} , \quad (27)$$

so that the intercept of the fatigue CFL line at the ordinate (I) or $I_{(CC)}$ for C-C loading is found to be

$$I_{(CC)} = S_{r1C}\sigma_{a,r1C} - S_{R(CC)}\sigma_{mean,r1C} \quad (28)$$

Therefore,

$$\sigma_a = I_{(CC)} + S_{R(CC)}\sigma_{mean} \cdot \quad (29)$$

2.3. Relationships of S-N Curve Parameters (α and β) with Stress Ratio (R)

Once S-N curve parameters for TRED are determined, S-N curve parameters (α and β) at different stress ratios can be theoretically calculated for prediction of S-N curves by establishing a relationship of α and β with stress ratio (R).

The damage rate $\left(\partial D_f / \partial N_f\right)$ [see Equation (2)] near the static strength $(\sigma_{uT}\ or\ \sigma_{uC})$ on log-log plot for $\partial D_f / \partial N_f$ versus $\sigma_{\max}$ tends to converge on a single point for different stress ratios (Figure **2b**). Accordingly, a relation between α and β independent of R using TRED for each loading segment is found to be:

$$\text{Log}\ \alpha = A + B\beta \quad (30)$$

where A and B are constants. The constants can be determined using the damage parameters of TRED in the case of for T-T loading:

$$B = \frac{\log \alpha_{(r0)} - \log \alpha_{(r1T)}}{\beta_{(r0)} - \beta_{(r1T)}} \quad (31a)$$

and

$$A = \log \alpha_{(r1T)} - B\beta_{(r1T)} \quad (31b)$$

where subscripts $r0$ and $r1T$ indicate for near R=0 and R=1 respectively. Note that the subscripts are consistent with those in Figure **2**. Similarly, other sets of constants for T-C, C-T, and CC loadings are also determined as listed in Table **1**.

Any radial line emanating from the origin at a given R in CFL diagram (Figure **2**) is given by

$$\sigma_a = \frac{1-R}{1+R}\sigma_{mean} \cdot \quad (32)$$

Table 1: Constants A and B

Loading	Constants
T-T	$B = \frac{\log \alpha_{(r0)} - \log \alpha_{(r1T)}}{\beta_{(r0)} - \beta_{(r1T)}}$, $A = \log \alpha_{(r1T)} - B\beta_{(r1T)}$
T-C	$B = \frac{\log \alpha_{(r\chi)} - \log \alpha_{(r0\prime)}}{\beta_{(r\chi)} - \beta_{(r0\prime)}}$, $A = \log \alpha_{(r0\prime)} - B\beta_{(r0\prime)}$
C-T	$B = \frac{\log \alpha_{(r\chi\prime)} - \log \alpha_{(r\infty)}}{\beta_{(r\chi\prime)} - \beta_{(r\infty)}}$, $A = \log \alpha_{(r\chi\prime)} - B\beta_{(r\chi\prime)}$
C-C	$B = \frac{\log \alpha_{(r\infty\prime)} - \log \alpha_{(r1C)}}{\beta_{(r\infty\prime)} - \beta_{(r1C)}}$, $A = \log \alpha_{(r\infty\prime)} - B\beta_{(r\infty\prime)}$

For T-T segment, a point (*e.g.* point *a* in Figure **2a**) on the radial line intersected by the fatigue CFL line for given N_f and R can be obtained by equating Equation (32) to Equation (14) such that,

$$\sigma_a = \frac{I_{(TT)}\,(1-\mathrm{R})}{1-R-S_{R(TT)}(1+\mathrm{R})}. \tag{33a}$$

Similarly, for T-C loading, C-T loading, and C-C loading, the fatigue CFLs are obtained for given N_f and R:

$$\sigma_a = \frac{I_{(TC)}(1-\mathrm{R})}{1-R-S_{R(TC)}(1+\mathrm{R})}; \tag{33b}$$

$$\sigma_a = \frac{I_{(CT)}(1-\mathrm{R})}{1-R-S_{R(CT)}(1+\mathrm{R})}; \quad \text{and} \tag{33c}$$

$$\sigma_a = \frac{I_{(CC)}(1-\mathrm{R})}{1-R-S_{R(CC)}(1+\mathrm{R})} \tag{33d}$$

respectively.

Accordingly, an arbitrarily chosen number of cycles ($N_f = N_{fc}$) for T-T and T-C loadings with a given R for σ_a is found from Equations (3) and (30) with $\sigma_{\max} = 2\sigma_a/(1-R)$;

$$N_{fc} = \frac{(\sigma_{uT})^{-\beta}}{10^{(A+B\beta)}(\beta-1)}\left[\left(\frac{2\sigma_a/(1-R)}{\sigma_{uT}}\right)^{1-\beta} - 1\right] + N_0 \tag{34a}$$

and for C-T and C-C loadings [note $\sigma_{min} = 2\sigma_a R/(1-R)$];

$$N_{fc} = \frac{|\sigma_{uC}|^{-\beta}}{10^{(A+B\beta)}(\beta-1)}\left(\left|\frac{2\sigma_a R/(1-R)}{\sigma_{uC}}\right|^{1-\beta} - 1\right) + N_0\,. \tag{34b}$$

Either of these two equations may be directly used for finding unknown β at a given R by numerically solving the equation with an arbitrarily chosen number of cycles (N_{fc}), and subsequently α can be determined according to Equation (30). A method determining α and β using Equation (34a or b) will be hereafter referred to as *one-point method*. This method may be efficient but the computing precision should be sometimes considered for accuracy because of the process involving both high powered numbers and small numbers. Table **2** lists formulas sequentially as a practical procedure for the one-point method calculation of T-T loading. For other loadings, the procedure in Table **2** can be used by replacing subscripts in equations with appropriate ones.

Table 2: One-Point Method for T-T Loading - One of Possible Sequences of Theoretical Calculation for Finding α and β at Different Stress Ratios

Sequence	Description	Expressions for Calculation
1	Damage parameters α and β for two sets of reference experimental data (TRED)	$\frac{\partial D_{fT}}{\partial N_f} = \alpha(\sigma_{max})^{\beta}$
2	Constants *A* and *B* using TRED for Log α = A+B β	$B = \frac{\log\alpha_{(r0)} - \log\alpha_{(r1T)}}{\beta_{(r0)} - \beta_{(r1T)}}$ and then $A = \log\alpha_{(r1T)} - B\beta_{(r1T)}$
3	Slopes of radial lines of TRED in CFL diagram	$S_{r0} = \frac{1-R_{r0}}{1+R_{r0}}$ and $S_{r1T} = \frac{1-R_{r1T}}{1+R_{r1T}}$
4	Two sets of mean stress values at given two values of N_f (*e.g.* $N_f = N_{f1} = 10^3$ and $N_{f2} = 10^5$ cycles) for TRED	$\sigma_{mean,r0}$ and $\sigma_{mean,r1T}$ using $\sigma_{mean} = (1+R)\sigma_{max}/2$ and $\sigma_{max} = \sigma_{uT}\left(\frac{\alpha(\beta-1)(N_f+N_0)}{(\sigma_{uT})^{-\beta}} + 1\right)^{\frac{1}{1-\beta}}$
5	Slope of fatigue CFL line, $S_{R(TT)}$, and intercept, $I_{(TT)}$, at the constant $N_{f(c)}$ for TRED	$S_{R(TT)} = \frac{S_{r0}\sigma_{mean,r0} - S_{r1T}\sigma_{mean,r1T}}{\sigma_{mean,r0} - \sigma_{mean,r1T}}$ and $I_{(TT)} = S_{r1T}\sigma_{mean,r1T} - S_R\sigma_{mean,r1T}$
6	Stress amplitude (σ_a) for given N_f and R	$\sigma_a = \frac{I_{(TT)}\,(1-\mathrm{R})}{1-R-S_{R(TT)}(1+\mathrm{R})}$
7	S-N curve parameter β numerically using a chosen constant value of $N_f (= N_{FC})$ for a given R	$N_{fc} = \frac{(\sigma_{uT})^{-\beta}}{10^{(A+B\beta)}(\beta-1)}\left[\left(\frac{2\sigma_a/(1-R)}{\sigma_{uT}}\right)^{1-\beta} - 1\right] + N_0$
8	S-N curve parameter α	$\mathrm{Log}\,\alpha = A + B\beta$
9	Polynomial functions for further applications	$\alpha = f(R)$ and $\beta = f(R)$

Another method for finding unknown β, which will be hereafter referred to as *two-point method*, can be found if we want to avoid the weakness of one-point method. This method is to utilise the linearity of the damage rate (Figure **2b**) without solving the equation numerically. It may start by choosing appropriate two numbers of cycles *i.e.* $N_f = N_{f1}$ (*e.g* 1000cycles) and N_{f2} ($>N_{f1}$ *e.g* 10^5cycles) for two points a and b as shown schematically for T-T loading in Figure **2**. The two points in CFL diagram (Figure **2a**) correspond to σ_{max1} and σ_{max2} ($\sigma_{max1} > \sigma_{max2}$) respectively in a diagram of log dD_f/dN_f versus log σ_{max} (Figure **2b**), which may be obtained from [note $\sigma_{\max} = 2\sigma_a/(1-R)$],

$$\sigma_{max} = \frac{2I}{1-R-S_R(1+R)}, \tag{35}$$

for a given *R* at which unknown *β* is to be found. Once $\sigma_{\max 1}$ and σ_{max2} are obtained, another set of corresponding two values of $\Delta D_f/\Delta N_f$ (*i.e.* $\Delta D_{f1}/\Delta N_f$ and $\Delta D_{f2}/\Delta N_f$) can be obtained (Figure **2b**) using

$$\frac{\Delta D_f}{\Delta N_f} = \frac{\Delta(1-\frac{\sigma_{max}}{\sigma_{uT}})}{\Delta N_f}. \tag{36}$$

where $\Delta N_f = (N_{f1} + \frac{1}{2}\Delta N_f) - (N_{f1} + \frac{1}{2}\Delta N_f)$ or $\Delta N_f = (N_{f2} + \frac{1}{2}\Delta N_f) - (N_{f2} + \frac{1}{2}\Delta N_f)$, $\Delta D_{f1} = D_{f1(H)} - D_{f1(L)}$ or $\Delta D_{f2} = D_{f2(H)} - D_{f2(L)}$, $D_{f1(H)} = 1 - \sigma_{max1(H)}/\sigma_{uT}$ at $N_{f1(H)} = N_{f1} + \frac{1}{2}\Delta N_f$ or $D_{f2(H)} = 1 - \sigma_{max2(H)}/\sigma_{uT}$ at $N_{f2(H)} = N_{f2} + \frac{1}{2}\Delta N_f$, $D_{f1(L)} = 1 - \sigma_{max1(L)}/\sigma_{uT}$ at $N_{f1(L)} (= N_{f1} - \frac{1}{2}\Delta N_f)$ or $D_{f2(L)} = 1 - \sigma_{max2(L)}/\sigma_{uT}$ at $N_{f2(L)} (= N_{f2} - \frac{1}{2}\Delta N_f)$. In numerical calculation, $\Delta N_f = N_{f1}/100$ or $\Delta N_f = N_{f2}$ /100 may be sufficiently accurate. From the diagram (Figure **2b**), we find,

$$\beta = \frac{\log\left(\frac{\Delta D_{f1}}{\Delta N_f}\right) - \log\left(\frac{\Delta D_{f2}}{\Delta N_f}\right)}{\log(\sigma_{max1}) - \log(\sigma_{max2})}. \tag{37}$$

Table **3** lists formulas sequentially as a practical procedure for the two-point method calculation of T-T loading. For other loadings, the procedure in Table **3** can be used by replacing subscripts in equations with appropriate ones.

For further applications, theoretical data for α and β may be obtained as functions of stress ratio (R) for curve fitting of the following polynomial equations with an adequate polynomial order n (Microsoft Excel is sufficiently capable for this process):

$$\log \alpha = a_{\alpha(n)}R^n + a_{\alpha(n-1)}R^{n-1} + a_{\alpha(n-2)}R^{n-2} + \cdots + a_{\alpha(n-n)}R^{n-n} \tag{35}$$

and

$$\beta = a_{\beta(n)}R^n + a_{\beta(n-1)}R^{n-1} + a_{\beta(n-2)}R^{n-2} + \cdots + a_{\beta(n-n)}R^{n-n}, \tag{36}$$

where a_α and a_β are polynomial coefficients.

3. VERIFICATION AND DISCUSSION

The accuracy of S-N curve predictions at various stress ratios entirely depends on the linearity of CFL lines and the accuracy of S-N curve model.

For T-T loading (or for $0 \le R < R_{r0} < R \le R_{r1T} \le R < 1$ in Figure **2**), unidirectional carbon fibre reinforced composites with σ_{uT} =52 MPa obtained for 50°C by Miyano and Nakada [31] at $R = R_{r0}$ =0.05 and R_{r1T} =0.9 were employed as TRED and another experimental data set obtained at R=0.5 was used for comparing

Table 3: One of Possible Sequences of Theoretical Calculation for Finding *α* and *β* at Different Stress Ratios Using Two-Point Method for T-T Loading

Sequence	Description	Expressions for Calculation
Same Sequence as one-Point Method for Sequence Steps1-5.		
6	For a given *R*, $\log \sigma_{\max}$ and then, corresponding $\log \frac{\Delta Df}{\Delta Nf}$ at $N_{f1} \pm \frac{1}{2}\Delta Nf$ and $N_{f2} \pm \frac{1}{2}\Delta Nf$ (where ΔNf is an arbitrary value chosen for numerical calculation)	$\sigma_{max} = \frac{2I_{(TT)}}{1-R-S_{R(TT)}(1+R)}$ and $\frac{\Delta D_f}{\Delta N_f} = \frac{\Delta(1-\frac{\sigma_{max}}{\sigma_{uT}})}{\Delta N_f}$
7	Parameter *β* for the given R	$\beta = \frac{\log\left(\frac{\Delta D_{f1}}{\Delta N_f}\right) - \log\left(\frac{\Delta D_{f2}}{\Delta N_f}\right)}{\log(\sigma_{max1}) - \log(\sigma_{max2})}$
Same sequence as one-point method for sequence steps 8-9.		

with theoretical prediction. According to the procedure given in Table **2**, the fitting/damage parameters in Equation (3) were found: logα=−38.61 and β=21.54 for R_{r0} =0.05; logα=77.14 and β=43.96 for R =0.5; and logα=136.79 and β=78.95 for R_{r1T} =0.9.The predicted S-N curve for R=0.5 is shown in Figure **3a** in comparison with a fitted S-N curve for experiment data. Also, Figure **3b** shows a CFL diagram, in which data points were taken from the fitted S-N curves of experiment data, and the linear fatigue CFL lines represented by the dashed lines for prediction. It is seen that the fatigue CFL lines tend to deviate a little from the data points at high values of N_f. This minor discrepancy, however, may be expected because of: (a) the sensitivity of N_f to the applied peak stress (σ_{max}) at high stress ratios (R>0.5); and (b) the 3-point bending testing method for the obtained experimental data generating a relatively high scatter compared to the uniaxial testing.

To find α and β by curve fitting as functions of R, a range of values at various stress ratios were theoretically calculated using the one-point method, and listed in Table **4**, and plotted in Figure **4** with TRED. Figure **4a** shows the damage rate as a function of applied peak stress on log-log scale. As expected, the fitted lines for TRED converge on a point. Also, a linear relationship between log α and β was found to be

$$\log \alpha = -1.780 - 1.710\,\beta \qquad (37)$$

with a correlation coefficient (cc) of 1.000 as shown in Figure **4b**.

The data in Table **4** is plotted in Figure **4c** and **d** and the following polynomial equations with a correlation coefficient (cc) of 1.000 for both were obtained:

$$\log \alpha = -503.67R^5 + 872.74R^4 - 635.84R^3 + 166.66R^2 - 52.333R - 36.33 \qquad (38a)$$

and

$$\beta = 294.52R^5 - 510.33R^4 + 371.8R^3 - 97.452R^2 + 30.601R + 20.203. \qquad (38b)$$

Table 4: Damage Parameters of Unidirectional Carbon Fibre Reinforced Composites Predicted with TRED Obtained at *R*=0.05 and 0.9 from on-Point Method for T-T Loading

Stress ratio (*R*)	Log *α*	*β*
0.05	-38.61	21.54
0.2	-43.90	24.63
0.3	-48.43	27.28
0.4	-54.10	30.60
0.5	-61.40	34.86
0.6	-71.10	40.54
0.7	-84.60	48.43
0.8	-104.54	60.09
0.9	-136.79	78.95

For T-C loading applicable for a stress ratio range $\chi \le R \le 0$, data sets for unidirectional carbon/epoxy

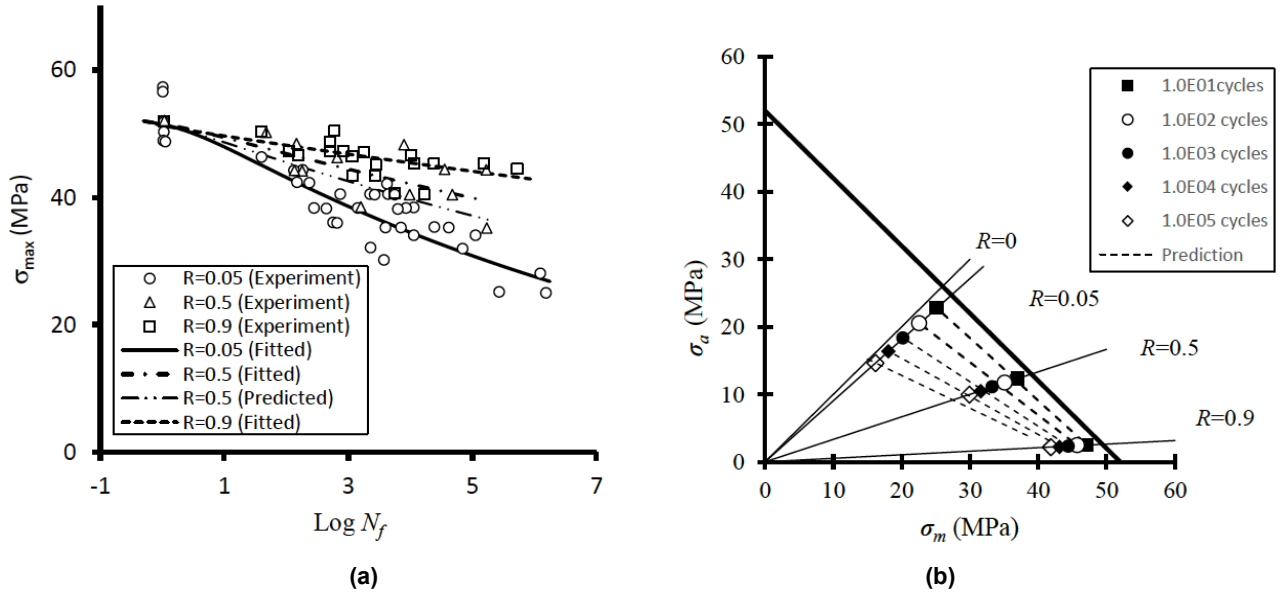

Figure 3: T-T loading with experimental data for fibre reinforced composites with σ_{uT}=52 MPa (Miyano and Nakada, 1995) and prediction for R=0.5: (**a**) S-N behaviour; and (**b**) CFL diagram.

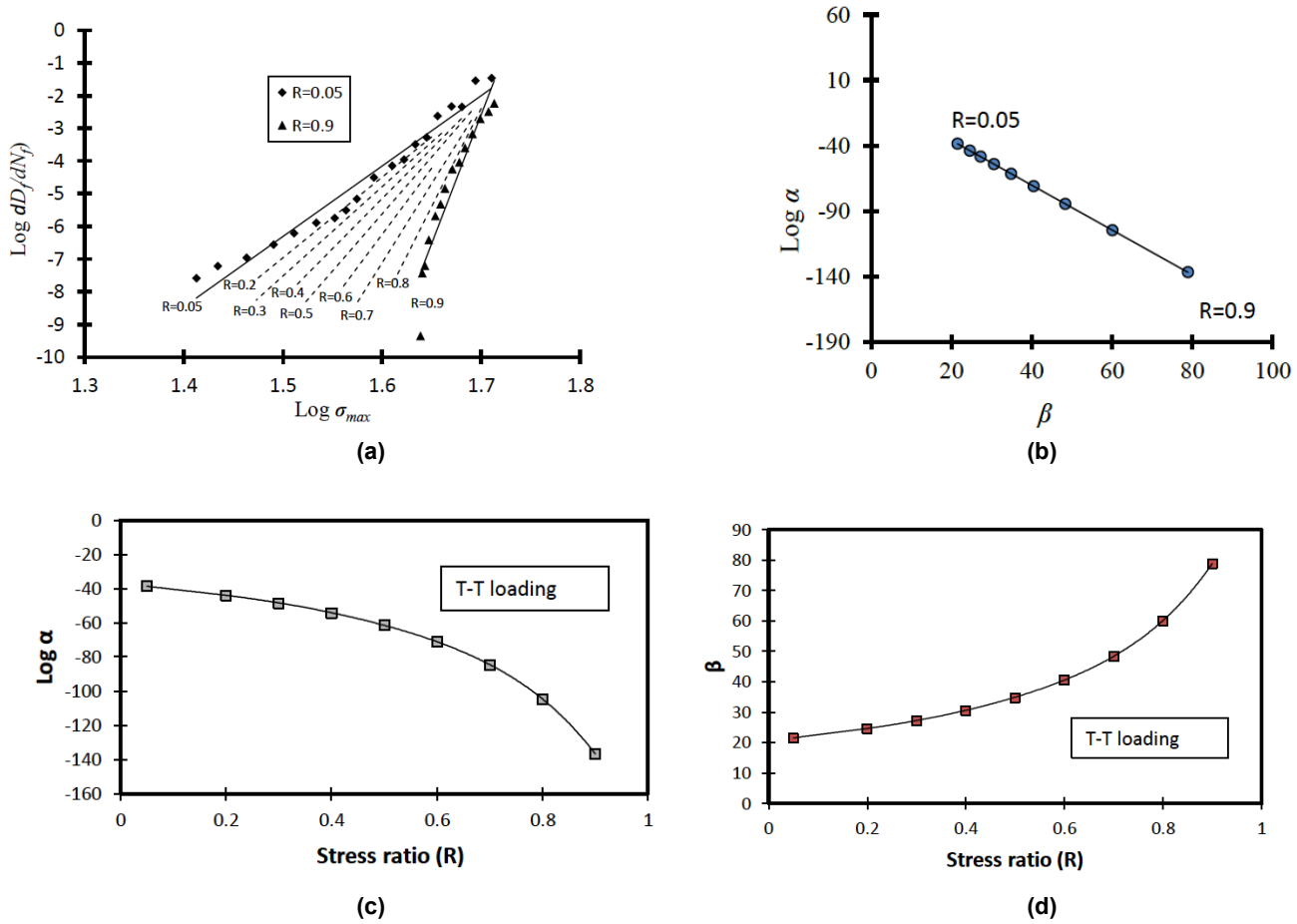

Figure 4: Damage rate and parameters (α and β) of TRED (Miyano and Nakada, 1995), and predictions obtained from one-point method for T-T loading: (**a**) $\log \Delta D_f/\Delta D_f$ versus log σ_{max}; (**b**) linear relationship between log α and β; (**c**) log α as a function of R ; and (**d**) β as a function of R.

laminate with transverse strengths σ_{uT}=30.1 MPa and σ_{uC}=154.0 MPa obtained by Kawai and Itoh [26] at R= 0.1, −1 and −5.12 were employed for verification. The two stress ratios (0.1 and −5.12) were used for TRED and the other R=−1 for comparing with prediction for $\chi \leq R \leq R_{rx} < R < R_{r0} \leq R \leq 0$ (Figure **5a**). The data set for R=−5.12 was used as $R = R_{rx} = x$ but the data set for R= 0.1 was not directly used as R_{r0} because it is from T-T loading segment but used to obtain an S-N curve at R=0 by extrapolation using two points, σ_{uT} and data point at R=0.1, for each data point at R=0. Thus, the obtained data set was used for R=0. The use of σ_{uT} for the extrapolation in this case may be acceptable because of the proximity of R=0.1 to R=0 (Figure **5b**) unlike the case of T-T loading. Fitting/damage parameters extrapolated for $R_{r0} = 0$ using the data for R=0.1 were found to be log α=–21.607 and β=13.342; and log α =−11.950 and β=6.716 for R_{rx} =−5.12. Eventually, using the reference data for R_{rx} and R_{r0} fitting/damage parameters for R=–1 were predicted to be log α =–17.146 and β=10.217 and its S-N curve is shown in Figure **5a**. The predicted S-N curve for R=–1 appears to be in good agreement with experimental results. Figure **5b** shows a CFL diagram in which data points are plotted from obtained S-N curves. Some deviation at low cycles (10^4 and 10^5) are noticeable but the actual experiment data points are in agreement with the calculated values. The predicted values obtained from the one-point method for other stress ratios are listed in Table **5** and graphically shown in Figure **6a**. Also, a linear relationship between logα and β was found to be

$$\log \alpha = 1.688 - 1.746\beta \quad (39)$$

with a correlation coefficient (cc) of 1.000 as shown in Figure **6b**. The following polynomial equations (Figure **6c** and **d**) were found as functions of R:

$$\log \alpha = -0.0066R^3 - 0.1299\,R^2 - 1.4963\,R - 21.606 \quad (40a)$$

and

$$\beta = 0.0038R^3 + 0.0744\,R^2 + 0.857\,R + 13.341 \quad (40b)$$

with a cc of 1.000 for both equations.

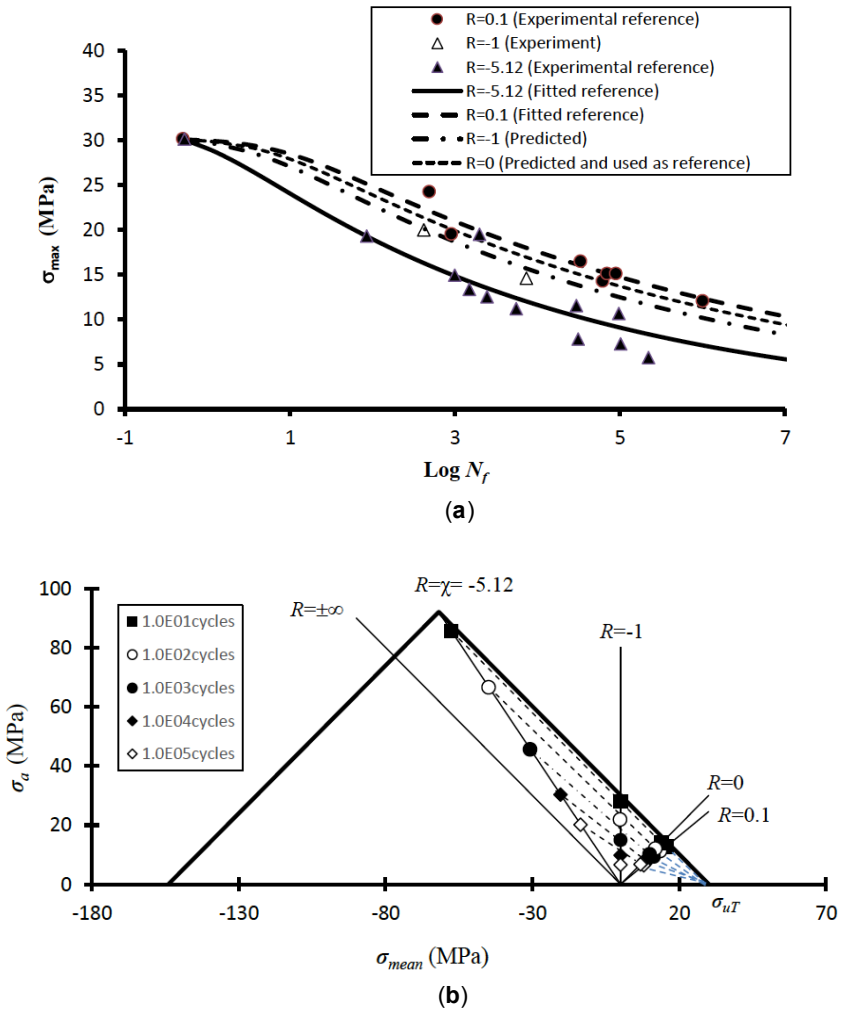

Figure 5: T-C loading with experimental data for unidirectional carbon/epoxy laminate $[90]_{16}$ with strengths σ_{uT}=30.1 MPa and σ_{uC}=154.0 MPa obtained for R=0.1, −1 and −5.12 (Kawai and Itoh, 2014): (**a**) S-N behaviour - the fitted line at R=0 was predicted using R=0.1 from T-T loading and then used as a reference data for S-N curve prediction, and subsequently S-N curve for R=−1 was predicted using two reference data sets at R=0 and −5.12.; and (**b**) CFL diagram.

Table 5: Damage Parameters Predicted with Reference Fatigue Data Sets for R=−5.12 and 0 for T-C Loading - Data Set for R=−5.12 was Experimentally Obtained and the Data Set for R=0 was Predicted Using Data for R=0.1

Stress ratio (R)	Log α	β
-5.12	-16.47	10.40
-4	-17.27	10.86
-3	-18.11	11.34
-2	-19.08	11.90
-1	-20.23	12.55
0	-21.61	13.34

For both C-C and C-T loadings, experimental data sets for unidirectional carbon/epoxy laminate $[0]_{16}$ with strengths σ_{uC}= 807MPa and σ_{uT}= 1887MPa obtained by Kawai and Itoh [26] were employed for verification.

For C-C loading applicable for a stress ratio range $+\infty \geq R \geq 1$, two experimental data sets obtained at R=10 and 2 are given with others in Figure **7a**. The data set for R=10 was used as for $R_{r\infty}$', and the experimental data set for R=2 was used for comparing with one point method prediction. The compressive strength (σ_{uC}) point was used as an approximate CFL line end point of R_{r1C} =1 for $+\infty \geq R > R_{r\infty} > R > R_{r1C} > 1$ without another reference experimental data set for R_{r1C} given that CFL lines passing through the experimental data points are close to each other (Figure **7b**). The predicted S-N curve for R=2 is in good agreement with the experimental data. Further predictions for other stress ratios were made and fitting/damage parameters are listed in Table **6** and graphically shown in Figure **8a**. Also, a linear relationship between $\log\alpha$ and β is found to be

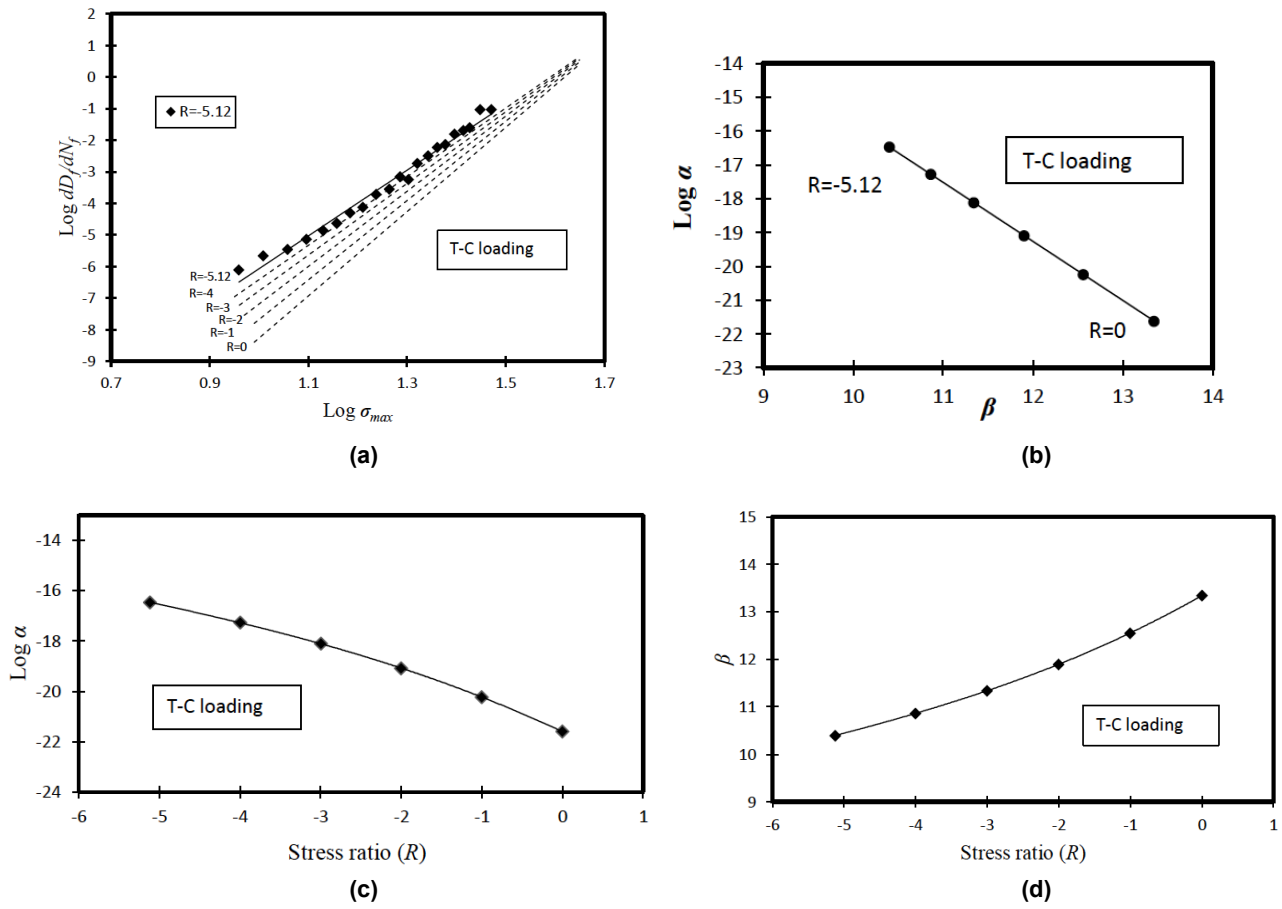

Figure 6: Damage rate and parameters (α and β) of TRED, and predictions obtained from one-point method for T-C loading: (**a**) log $\Delta D_f/\Delta D_f$ versus log σ_{max}; (**b**) linear relationship between log α and β; (**c**) log α as a function of R; and (**d**) β as a function of R.

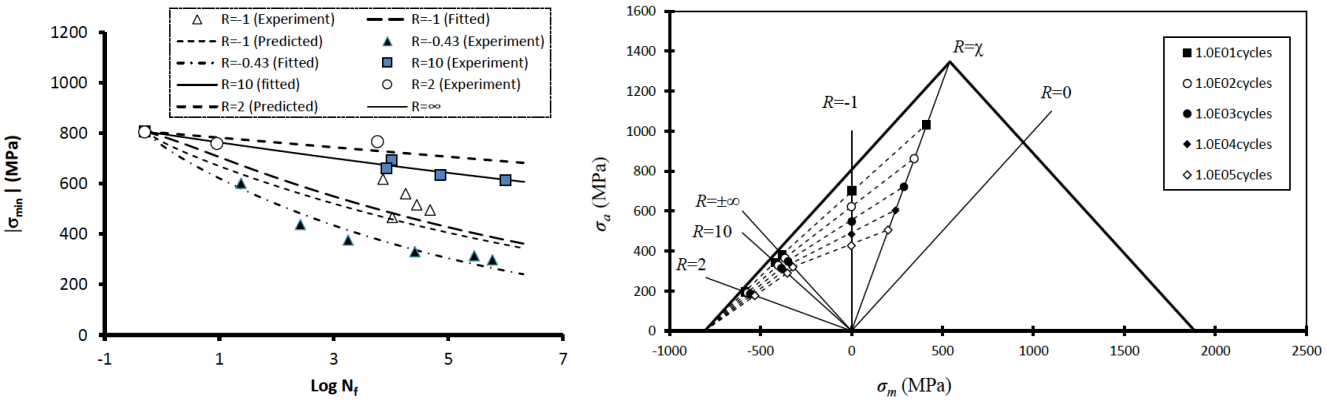

Figure 7: Experimental data for unidirectional carbon/epoxy laminate $[0]_{16}$ with strengths σ_{uC}= 807MPa and σ_{uT}= 1887MPa obtained for R=2 and 10 under C-C loading and for R=-0.43 and -1 under C-T loading (Kawai and Itoh, 2014): (**a**) fitted and predicted S-N curves – practically no difference in fitted S-N curve between R=10 and ∞ is seen; and (**b**) CFL diagram for both C-C and C-T loadings.

$$\log \alpha = -1.4221 - 2.9074\,\beta \quad (41)$$

with a cc of 1.000 as shown graphically in Figure **8b**. The following polynomial equations as functions of R for C-C loading were found (Figure **8c** and **d**):

$$\log \alpha = -0.0105R^6 + 0.4263R^5 - 7.068R^4 + 61.453R^3 - 297.44R^2 + 773.66R - 1045.4 \quad (42a)$$

and

$$\beta = 0.0036R^6 - 0.1466R^5 + 2.431R^4 - 21.137R^3 + 102.3R^2 - 266.1R + 359.08 \quad (42b)$$

with a cc of 1.000 for both equations.

Table 6: Damage Parameters Predicted with a Reference Fatigue Data Set for *R*=10 for C-C and C-T Loadings

Loading	Stress Ratio (*R*)	Log *α*	*β*
C-C	2	-296.38	101.45
	3	-218.57	74.688
	4	-193.13	65.936
	5	-180.52	61.600
	6	-172.99	59.011
	7	-168.01	57.296
	8	-164.44	56.07
	9	-161.78	54.439
	10	-159.70	54.439
C-T	-0.43	-41.074	13.910
	-1	-60.588	20.483
	-2	-82.350	27.899
	-3	-96.210	32.641
	-4	-105.85	35.944
	-5	-113.62	38.615
	-6	-118.38	40.244
	-7	-122.69	41.723
	-8	-126.18	42.922
	-9	-129.07	43.915
	-10	-131.50	44.750
	-∞	-159.69	54.438

For C-T loading applicable for a stress ratio range, data set for $R = x = R_{rx'} = -0.43$ was employed as a reference experimental data for $-\infty \le R_{r\infty} < R < R_{rx'} \le X$. Also, another experimental data set for $R=-1$ was employed for comparing with two point method prediction. A reference data set for $R_{r\infty}$ was predicted

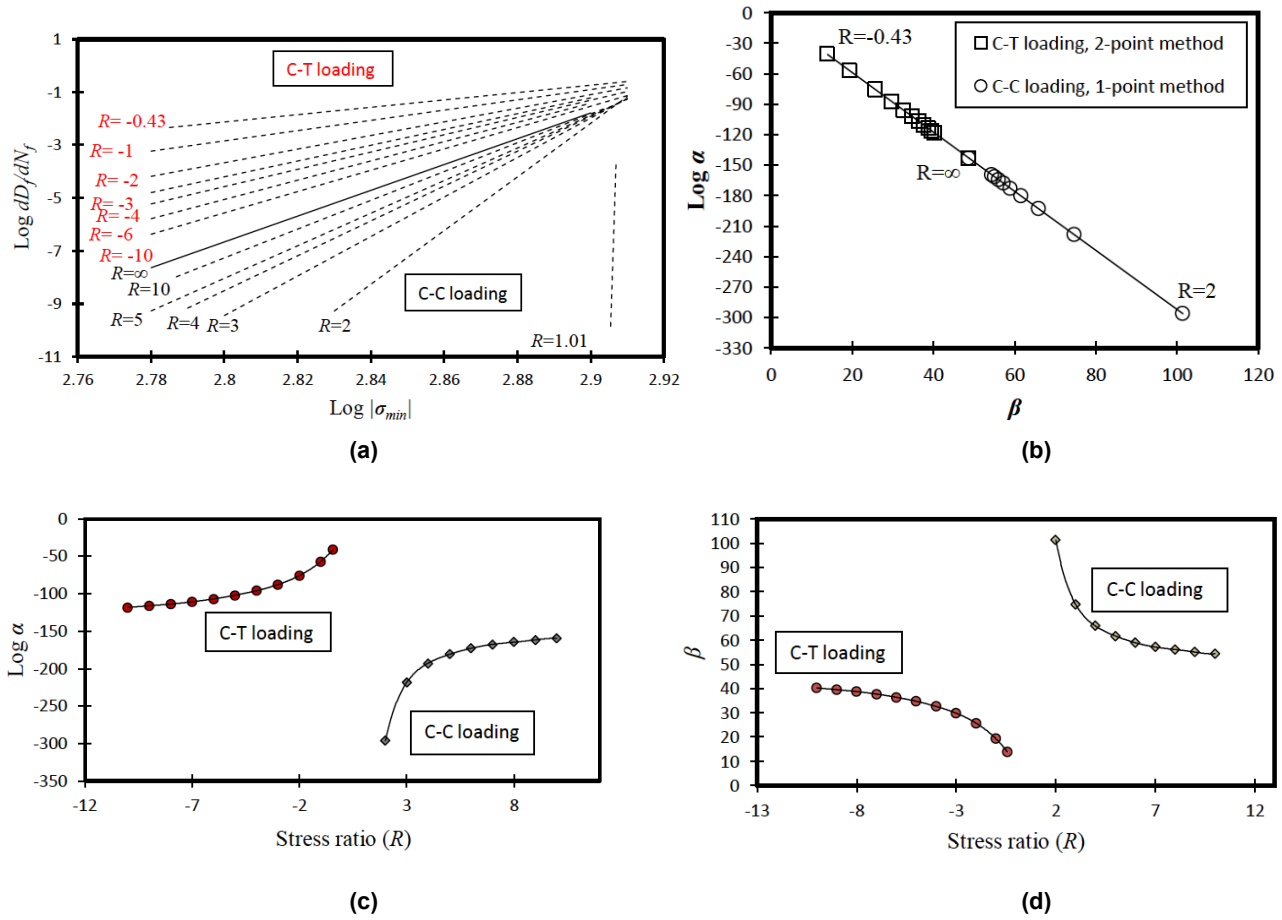

Figure 8: Damage rate and parameters (α and β) predicted using TRED (Kawai and Itoh, 2014) for C-C and C-T loadings: (**a**) log $\Delta D_f/\Delta D_f$ versus log σ_{max}; (**b**) linear relationship between log *α* and *β*; (**c**) log *α* as a function of R; and (**d**) *β* as a function of R.

under C-C loading and its S-N curve is shown with others in Figure **7a**. Eventually, prediction of S-N curve made for $R=-1$ appears to be in good agreement with the fitted curve of experimental data as shown in Figure **7a**. Also CFL diagram (Figure **7b**) confirms the good agreement between prediction (dashed line) and data points from the fitted S-N curve for $R=-1$. Also, a linear relationship between $\log\alpha$ and β is found to be

$$\log \alpha = -0.3162 - 2.9301\beta \quad (43)$$

with a cc of 1.000 as shown in Figure **8b**. Further predictions for other stress ratios under C-T loading were made and fitting/damage parameters are listed in Table **6** and graphically shown in Figure **8b** with those of C-C loading. The following polynomial equations were found as functions of *R* for C-T loading (Figure **8c** and **d**):

$$\log \alpha = 0.003R^5 + 0.0998R^4 + 1.3174R^3 + 9.1605R^2 + 38.655R - 26.175 \quad (44a)$$

and

$$\beta = -0.001R^5 - 0.0341R^4 - 0.4496R^3 - 3.1263R^2 - 13.192R + 8.8254 \quad (44b)$$

with a cc of 1.000 for both equations.

4. CONCLUSION

A new practical procedure has been studied to predict S-N curves at various stress ratios. The theoretical and experimental characteristics of the constant fatigue life (CFL) diagram were clarified for capability and limitations, and dependence of experimental fatigue behaviour. Mathematical relationships between linear CFL lines and fatigue damage parameters were successfully derived. As a result, the Kim and Zhang S-N curve model was successfully dovetailed with the linear CFL lines to predict S-N curves for the whole range of stress ratios. Theoretical predictions of fatigue life based on the mathematical relationships were verified with the experimental data.

REFERENCES

[1] Kim HS. Mechanics of Solids and Fracture, 3rd ed. Bookboon, London 2018. ISBN 978-87-403-2393-1.

[2] Kitagawa H, Takashima S. Application of fracture mechanics to very small fatigue cracks or the cracks in the early stage. Proceedings of the Second International Conference on Mechanical Behavior of Materials, American Society for Metals, Materials Park, Boston, MA, USA, 16-20 August 1976; pp. 627-631.

[3] Eskandari H, Kim, HS. A Theory for mathematical framework and fatigue damage function for the S-N plane. In Fatigue and Fracture Test Planning, Test Data Acquisitions, and Analysis; ASTM STP1598; Wei, Z., Nikbin, K., McKeighan PC, Harlow DG. Eds.; ASTM International: West Conshohocken, PA, USA, 2017; pp. 299-336. https://doi.org/10.1520/STP159820150099

[4] Burhan I, Kim HS. S-N curve models for composite materials characterisation: an evaluative review, Journal of Composites Science 2018; 2: 1-29. https://doi.org/10.3390/jcs2030038

[5] Gerber WZ. Bestimmung der zulassigen Spannungen in Eisen-Constructionen. [Calculation of the allowable stresses in iron structures]. Z Bayer Arch. Ing. Ver. 1874; 6: 101-110.

[6] Weyrauch PJJ. Strength and Determination of the Dimensions of Structures of Iron and Steel with Reference to the Latest Investigations, 3rd ed.; Du Bois, A.J., Translator; John Wiley and Sons: New York, NY, USA 1877.

[7] Goodman J. Mechanics Applied to Engineering, 1st ed.; Longmans, Green and Co.: London, UK 1899.

[8] Soderberg CR. Factor of safety and working stress. Trans. Am. Soc. Test Matls. 1930; 52: 13-28.

[9] Basquin OH. The exponential law of endurance test. ASTM STP 1910, 10, 625-630.

[10] WeibullW. The statistical aspect of fatigue failures and its consequences. In Fatigue and Fracture of Metals; Massachusetts Institute of Technology; John Wiley & Sons: New York, NY, USA, 1952; pp. 182-196.

[11] Sendeckyj GP. Fitting models to composite materials fatigue data. In Test Methods and Design Allowables for Fibrous Composites; ASTM STP 734; Chamis, C.C., Ed.; ASTM International: West Conshohocken, PA, USA, 1981; pp. 245-260. https://doi.org/10.1520/STP29314S

[12] Bond IP. Fatigue life prediction for GRP subjected to variable amplitude loading, Composites: Part A 1999; 30: 961-970. https://doi.org/10.1016/S1359-835X(99)00011-1

[13] Passipoularidis VA, Philippidis TP, A study of factors affecting life prediction of composites under spectrum loading, International Journal of Fatigue 2009; 31: 408-417. https://doi.org/10.1016/j.ijfatigue.2008.07.010

[14] Adam T, Fernando G, Dickson RF, Reiter H, Harris B. Fatigue life prediction for hybrid composites. Int J Fatigue 1989; 11(4): 233-7. https://doi.org/10.1016/0142-1123(89)90306-X

[15] Kawai M, Koizumi M. Nonlinear constant fatigue life diagrams for carbon/ epoxy laminates at room temperature, Composites: Part A 2007; 38: 2342-2353. https://doi.org/10.1016/j.compositesa.2007.01.016

[16] Sendeckyj G P. Constant life diagram - a historical review, International Journal of Fatigue 2001; 23: 347-353. https://doi.org/10.1016/S0142-1123(00)00077-3

[17] Kawai M. Fatigue life prediction of composite materials under constant amplitude loading, Chapter 6, in Fatigue life prediction of composites and composite structures edited by A. P. Vassilopoulos, Woodhead Publishing Limited, Oxford, Cambridge, New Delhi, 2010, p182. https://doi.org/10.1533/9781845699796.2.177

[18] Haigh BP. Experiments on the fatigue of brasses. J Inst Metals 1917; 18: 55-86. https://doi.org/10.1177/002205741708600114

[19] D'Amore A, Caprino G, Stupak P, Zhou J, Nicolais L. Effect of stress ratio on the flexural fatigue behaviour of continuous strand mat reinforced plastics, Science and Engineering of Composite Materials 1996; 5(1): 1-8. https://doi.org/10.1515/SECM.1996.5.1.1

[20] Vassilopoulos AP, Manshadi BD, Keller T. Piecewise non-linear constant life diagram formulation for FRP composite materials, International Journal of Fatigue 2010; 32: 1731-1738. https://doi.org/10.1016/j.ijfatigue.2010.03.013

[21] Poursartip A, Beaumont PWR. The fatigue damage mechanics of carbon fibre composite laminate: II-Life prediction. Compos Sci Techno 1986; 25: 283-299. https://doi.org/10.1016/0266-3538(86)90045-X

[22] Epaarachchi JA, Clausen PD. An empirical model for fatigue behavior prediction of glass fibre-reinforced plastic composites for various stress ratios and test frequencies. Compos. Part A Appl. Sci. Manuf. 2003; 34: 313-326. https://doi.org/10.1016/S1359-835X(03)00052-6

[23] Weibull W. Chapter VIII, Presentation of Results. In Fatigue Testing and Analysis of Results; Pergaman Press: Oxford, UK; London, UK; New York, NY, USA; Paris, France 1961. https://doi.org/10.1016/B978-0-08-009397-0.50012-6

[24] Kim HS, Zhang J. Fatigue damage and life prediction of glass/vinyl ester composites, Journal of Reinforced Plastics and Composites 2001; 20: 834-848. https://doi.org/10.1177/073168401772678959

[25] Harris B, Gathercole N, Lee JA, Reiter H, Adam T. Philosophical Transactions: Mathematical, Physical and Engineering Sciences Jun. 15, 1997; 355(1727): 1259-1294. https://doi.org/10.1098/rsta.1997.0055

[26] Kawai M, Itoh N. A failure-mode based anisomorphic constant life diagram for a unidirectional under off-axis fatigue loading at room temperature. Journal of Composite Materials 2014; 48(5): 571-592. https://doi.org/10.1177/0021998313476324

[27] Ibrahim B, Kim HS, Thomas S. A refined S-N curve model, In: International Conference on Sustainable Energy, Environment and Information (SEEIE 2016), Bangkok, Thailand, 2016, pp.412-416, doi:10.1017/CBO9781107415324.004; AMSME-E107, 23/34-35 Traimit Road, Taladnoy, Bangkok 10100, Thailand.

[28] Eskandari H, Kim HS. A theory for mathematical framework of fatigue damage on S-N plane, Key Engineering Materials 2015: 627:117-120. https://doi.org/10.4028/www.scientific.net/KEM.627.117

[29] Vassilopoulos AP, Manshadi BD, Keller T. Influence of the constant life diagram formulation on the fatigue life prediction of composite materials, International Journal of Fatigue 2010; 32: 659-669. https://doi.org/10.1016/j.ijfatigue.2009.09.008

[30] Gamstedt EK, Sjogren BA. Micromechanisms in tension-compression fatigue of composite laminates containing transverse plies. Compos Sci Technol 1999; 59: 167-178. https://doi.org/10.1016/S0266-3538(98)00061-X

[31] Miyano Y, Nakada M. Influence of stress ratio on fatigue behaviour in the transverse direction of unidirectional CFRPS, Journal of Composite Materials 1995; 29:1808-1822. https://doi.org/10.1177/002199839502901401

[32] Veazie DR, Gates TS. Compressive Creep of IM7/K3B Composite and the Effects of Physical Aging on Viscoelastic Behavior, Experimental Mechanics 1997; 37(1): 62-68. https://doi.org/10.1007/BF02328751

Received on 13-11-2019 Accepted on 10-12-2019 Published on 30-12-2019

DOI: https://doi.org/10.12974/2311-8717.2019.07.8

© 2019 Ho Sung Kim; Licensee Savvy Science Publisher.
This is an open access article licensed under the terms of the Creative Commons Attribution Non-Commercial License (http://creativecommons.org/licenses/by-nc/3.0/) which permits unrestricted, non-commercial use, distribution and reproduction in any medium, provided the work is properly cited.